Transl. Stroke Res. (2018) 9:135–145
DOI 10.1007/s12975-017-0563-1

ORIGINAL ARTICLE

Protective Effects of Autologous Bone Marrow Mononuclear Cells After Administering t-PA in an Embolic Stroke Model

Bing Yang[1] · Weilang Li[2] · Nikunj Satani[1] · Duyen M. Nghiem[1] · XiaoPei Xi[1] · Jaroslaw Aronowski[1] · Sean I. Savitz[1]

Received: 6 June 2017 / Revised: 9 August 2017 / Accepted: 10 August 2017 / Published online: 23 August 2017

Abstract Tissue plasminogen activator (t-PA) is the only FDA-approved drug for acute ischemic stroke but poses risk for hemorrhagic transformation (HT). Cell therapy has been investigated as a potential therapy to improve recovery after stroke by the modulation of inflammatory responses and the improvement of blood-brain barrier (BBB) integrity, both of which are associated with HT after t-PA. In our present study, we studied the effect of autologous bone marrow mononuclear cells (MNCs) in an embolic stroke model. We administered MNCs in a rat embolic stroke 2 h after administering t-PA. We observed that even though autologous MNCs did not alter the incidence of HT, they decreased the severity of HT and reduced BBB permeability. One possible mechanism could be through the inhibition of MMP3 released by astrocytes via JAK/STAT pathway as shown by our in vitro cell interaction studies.

Keywords Cellular therapy · Embolic stroke · Hemorrhagic transformation · Blood-brain barrier integrity · Reperfusion injury

✉ Bing Yang
Bing.Yang@uth.tmc.edu

[1] Institute for Stroke and Cerebrovascular Disease and Department of Neurology, McGovern Medical School, University of Texas Health Science Center (UTHealth) at Houston, Houston 77030, TX, USA

[2] Department of Neurology, Tongde Hospital of Zhejiang Province, Hangzhou, China

Introduction

Tissue plasminogen activator (t-PA) is the only FDA-approved drug for acute ischemic stroke. Despite the narrow time window of 4.5 h after stroke onset, a frequent limitation for t-PA treatment is the complication of intracerebral hemorrhagic transformation (HT). HT incidence occurs up to 40% after t-PA treatment. One possible reason for HT after t-PA is due to increased blood-brain barrier (BBB) permeability after early BBB disruption caused by cerebral ischemia in animal and clinical studies [1–4].

Cell therapy has demonstrated safety in both experimental animal stroke models as well as in stroke patients. However, questions remain on which cell type to administer and from which route for different types of stroke [5]. Autologous bone marrow-derived mononuclear cells (MNCs), as one type of cell-based therapy, have recently been shown to have potential benefits in the recovery after stroke by our team and other investigators [6–8] and is under active investigation as a potential new therapy in clinical trials [9–13]. Considering that most patients presenting in the first few hours after symptom onset to stroke centers are treated with t-PA, studying the effects of MNCs following t-PA treatment is clinically relevant. We previously reported that MNCs regulate serum inflammatory cytokine levels, modulating free radicals and reducing brain edema [14, 15], which are all regarded as potential factors associated with BBB disruption after stroke [16, 17]. In addition, MNCs have been found to reduce BBB disruption in a model of traumatic brain injury [18] and ICH stroke model [15]. Thus, we hypothesized that MNC treatment might improve BBB permeability and reduce HT induced by t-PA in ischemic stroke.

Challenge in using rodent model of stroke is the fact that results are not easily translatable clinically. More studies are required for use of stroke model which encompasses t-PA-induced

reperfusion and hemorrhagic transformation [19]. Similarity of our model to clinical stroke was the reason we employed a rodent embolic ischemic stroke model with t-PA treatment for studying effects of BBB impairment on HT. We treated ischemic animals with autologous MNCs or saline control. We compared the incidence and severity of HT and also assessed BBB permeability. To better understand the possible mechanisms underlying the effects of MNCs on the BBB, we also measured matrix metalloproteinase 3 (MMP-3) levels in serum, brain, and astrocytes. We report that autologous MNC delivery after stroke attenuates HT severity induced by t-PA.

Materials and Methods

Animals

Ninety male long-Evan rats (275–300 g) and three E18 pregnant rats were purchased from Harland Lab, USA. All rats were housed in a 12-h light/dark cycle and were given free access to water and food. All animal experiments and surgical procedures were approved by the University of Texas Health Science Center Animal Welfare Committee and followed National Institutes of Health guidelines and regulations.

Embolic Stroke Model

The embolic stroke model with t-PA treatment was generated as per the timeline shown in Fig. 1a, c.

Autologous Blood Clot Preparation Animals were anesthetized under 2% isoflurane; 200 μl arterial blood (autologous blood) was collected via a 27 gauge hypodermic needle via the tail artery and retained in 10 cm of PE-50 tubing after mixing with 40 μl of thrombin at 100 IU/ML for 2 h at room temperature. Afterwards, 5 cm of the PE-50 tubing-containing clot was then cut and attached to a syringe filled with saline. The clot was flushed out and cut to 10 mm length and soaked in saline for 22 h at 4 °C (Fig. 1b). The next day, a single clot (10 mm) was transferred to a modified PE-10 catheter with a 0.3-mm outer diameter filled with 20 μl saline for creating a rat embolic middle cerebral artery occlusion stroke model.

Embolic Middle Cerebral Artery Occlusion Animals were anesthetized with 2% isoflurane in 30% O_2, 70% N_2O by face mask. After creating a midline incision under the operating microscope, the left common carotid artery (CCA), the left external carotid artery (ECA), the left internal carotid artery (ICA), and the left pterygopalatine artery (PPA) were isolated and carefully separated from the adjacent vagus nerve. A 6–0 nylon suture was loosely tied at the origin of the ECA and another suture was ligated at the distal end of the ECA. The left CCA, ICA, and PPA were temporarily clamped using a curved microvascular clip (Codman & Shurtleff, Inc., Randolf, MA, USA). The pre-prepared modified PE-10 catheter with a 0.3-mm outer diameter containing an autologous blood clot was attached to a 100-μl Hamilton syringe and was introduced into the ECA lumen through a small puncture. The suture around the origin of the ECA was tightened around the intraluminal catheter to prevent bleeding, and the

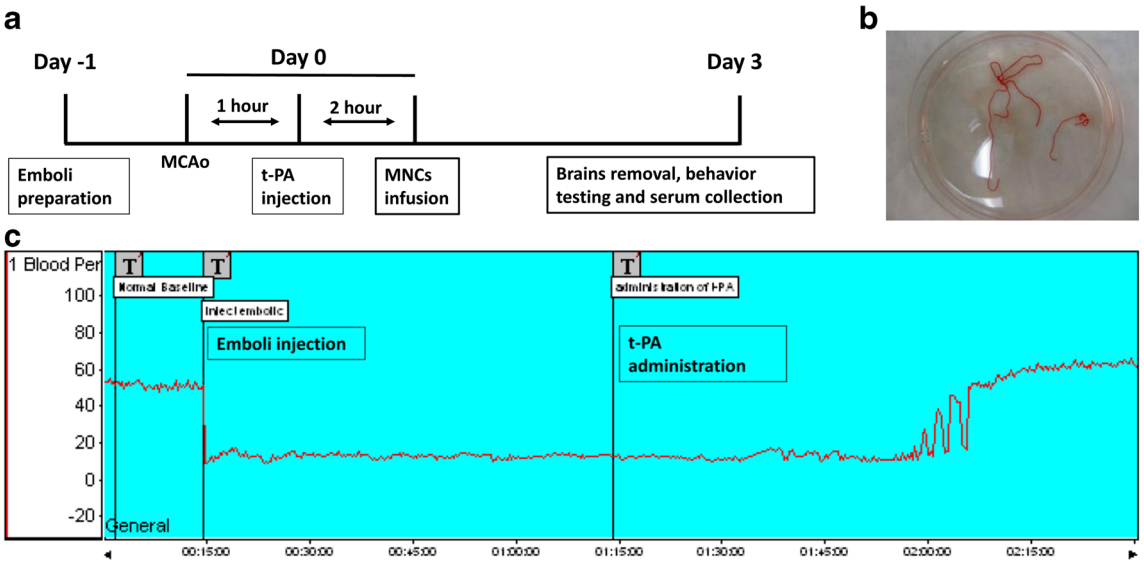

Fig. 1 **a** Schematic representation of the experimental groups and time line. **b** A picture of homologous blood clots (fibrin-rich) used to produce an embolic middle cerebral artery occlusion (MCAo) in adult rats. **c** A representative curve of cerebral blood flow (CBF) monitored by Laser Doppler Flowmetry (LDF). The 75% or more drop of CBF than baseline meant stroke by MCAo and more than 50% recovered CBF out of the total drop meant successful reperfusion caused by t-PA

microvascular clip on ICA was removed. The catheter was gently advanced from the ECA into the lumen of the ICA. When the end of the intraluminal catheter passed 2 to 3 mm from the origin of the MCA, the embolus was then gently injected through it. After injection of the embolus, the catheter was removed. The left ECA was ligated. The clip on CCA and PPA was released, and the skin incision was closed with applying Marcaine (0.25%) locally.

Thrombolytic Intervention with Recombinant t-PA At 1 h after embolism, recombinant t-PA (Genentech, USA) was dissolved in saline and administered intravenously at a dose of 10 mg/kg body weight with a 10% bolus and then followed by a 90% continuous infusion over 60 min by using an automatic injection pump via the right femoral vein. The dosage was chosen as reported previously [2, 20] and based on the different enzyme activity between human and animal models [21].

Monitoring on Cerebral Focal Blood Flow In the present study, the cerebral focal blood flow (CBF) was monitored during the entire process starting from the embolic MCAo up to the end of t-PA injection **(**Fig. 1c**)**. A probe of Laser Doppler Flowmeter was placed over the MCA perfusion territory (2 mm posterior and 6 mm lateral to bregma) as reported [8], and the perfusion curve was continuously recorded from baseline. Only those rats with 75% or more reduction from CBF baseline was confirmed as adequate focal cerebral ischemia and more than 50% recovery after t-PA was regarded as successful reperfusion.

Animal Groups and Autologous MNC Treatment

Rats with successful stroke and good re-perfusion after t-PA were randomly assigned into two groups: (1) received autologous MNC treatment and (2) received saline treatment. MNCs were collected and isolated right at 1 h after MCAo with the procedures we reported previously [14]. In the saline control group, a sham procedure was performed. At 2 h after t-PA infusion, rats were treated with autologous MNCs given at 1×10^7 cells/kg in 1 ml of saline intravenously (IV) via right femoral vein over 5 min. Control rats were administered 1 ml of saline IV only over 5 min [15].

Experiments were separated for different endpoints readout: (1) hemorrhage transformation and infarction size assessment, serum cytokines measurement, and the deficit evaluation; (2) evaluation of BBB integrity; and (3) immunohistochemistry assay with brain tissue and slices.

In another separate experiment, MNCs were labeled by Q-tracker 655 (Thermofisher, USA) according to the manufacture protocol before infusion only in t-PA treatment group. Three days later, the brains were harvested for MNC biodistribution assessment.

Hemorrhage Transformation and Infarction Size Assessment

At day 3 after stroke onset, rats were euthanized with 5% fatal isoflurane. The brains were removed and cut into six 2-mm-thick coronal sections in a cutting matrix. Brain sections were then stained with 2% 2,3,5-triphenyltetrazolium chloride (TTC) for 30 min at room temperature, followed by overnight immersion in 10% formalin. The sections were then scanned digitally and assessed by ImageJ. Visible hemorrhagic transformation was assessed from each section.

To provide more translatable assessment, we further categorized the subtype of hemorrhagic transformation using criteria from a human study [22, 23] on the significance of hemorrhage after t-PA. Four subtypes of hemorrhagic transformation were recognized: (1) hemorrhagic infarction 1 (HI-1), with scattered, heterogeneous petechiae along the margins of the infarct; (2) hemorrhagic infarction 2 (HI-2), with more confluent but still heterogeneous petechiae within the infarcted area; (3) parenchymal hematoma 1 (PH-1), with a homogeneous hematoma covering < 30% of the infarcted area and only mild space-occupying effect; and (4) parenchymal hematoma 2 (PH-2), with a dense hematoma > 30% of the lesion volume with significant space-occupying effect.

The infarct area was calculated from each section by ImageJ (NIH). The total area from six sections was added and then multiplied by the thickness (2 mm) to obtain the infarct volume. We used an indirect measure to correct the total infarct volume for edema. Corrected infarct area was calculated as follows:

$$measured\ infarct\ area \times \left[1-\left\{\frac{(ipsilateral\ hemisphere\ area-contralateral\ hemisphere\ area)}{contralateral\ hemisphere}\right\}\right]$$

Evaluation of BBB Integrity

The permeability of the BBB was determined by using Evans blue as reported [15]. Briefly, at day 3 after stroke onset, rats were given 4 ml/kg of 2% Evans blue (EB; Sigma, USA) solution intravenously via the femoral vein under 2% isoflurane. One hour later, after an intracardial perfusion of warm saline (37 °C), the rats were subsequently decapitated

and the brains were removed. Right and left hemispheres were separated and weighed. Then, both hemispheres were incubated in 5 ml formamide at 50 °C for 24 h. The concentration of dye extracted was determined at 620 nm using spectrophotometry (UV7500, Spectro Lab, England), and data was expressed as absorbance per gram of tissue.

Measurement of Neurological Deficit

Neurological deficits were recorded at day 3 after embolic stroke and determined using a 6-point scoring system modified [24] as follows: 0, no observable deficit; 1, forelimb flexion; 2, forelimb flexion plus decreased resistance to lateral push; 3, unidirectional circling; 4, unidirectional circling plus decreased levels of consciousness; and 5, death. Behavioral tests were carried out by an observer blind to the experimental groups.

Immunohistochemistry

At 3 days after MCAo and treatment, rats were perfused intracardially with ice-cold PBS. The brains were then harvested and snap frozen. In the cryostat, the brains were divided into 6 coronal pieces (2 mm, I to VI). Sections II to IV were cut onto slides and three coronal 10-μm cryosections were selected from each section, followed by fixation with 2% paraformaldehyde for 30 min at room temperature. After blocking for 2 h in 5% Donkey serum and 0.01% Triton-X 100 in PBS at room temperature, the cryosections were incubated with following primary antibodies: goat polyclonal anti-rat GFAP antibody (1:500, Abcam) and rabbit polyclonal anti-rat MMP3 (1:100, Abcam) overnight at 4 °C. Slides were then incubated with secondary antibodies conjugated to Alexa Fluor 488 or Alexa Fluor 568 (1:1000, Invitrogen) for 2 h at room temperature.

For GFAP and MMP3 positive cell analysis, 3 views were randomly selected from the peri-infarct region in each cryosection. The immunofluorescence signal was captured under the view with 400× magnification using fluorescence microscope equipped with charge-coupled device camera, and all immunopositive cells were analyzed using ImageJ software (NIH, Maryland, USA). Scale bar = 35 μm.

For GFAP and Q-tracker labeled MNCs, fluorescent images were collected with Zeiss LSM 780 confocal laser scanning microscopes (Carl Zeiss, Thornwood, NY) in the peri-infacrt region. All sections were imaged with dye-appropriate spectral acquisition parameters. 63× oil immersion objective with numerical apertures of 1.40 was used to collect images. Each channel (DAPI, 488, or 649) was scanned separately in sequential frame mode. Single optical sections were 0.3 μm. The images were analyzed as single optical sections and as stacks of optical sections projected along the *x*-, *y*-, or *z*-axes. Stacks were created using the Maximum Intensity Projection function within the Zen 2012 software. The IMARIS x64 7.6.3 software (BITPLANE) was used for orthogonal imaging. Images were processed with Photoshop for brightness and contrast adjustment. Scale bar = 10 μm.

Serum or Media Cytokine Measurements

Venous blood serum samples were collected at pre-stroke and day 3 after stroke. Media samples were collected from the well with co-culture after 24 h. Interleukin (IL)-1β, IL-10 (Thermo Scientific, USA), and MMP-3 levels were detected by ELISA according to the manufacturers' protocols.

Cell Culture

Primary Astrocyte Culture Primary astrocyte cultures were prepared from the cortex of neonatal (P1) rats according to the procedures described previously [25]. Briefly, forebrains were removed from skulls and placed in ice-cold HBSS (Invitrogen) with 10 mM HEPES. After careful dissection to remove the meninges, cortices were minced, dissociated by trituration and vortexing, passed through sterile nylon sieves (100, 70, and 10 μM), and then plated in 24-well plates on poly-D-lysine-coated glass coverslips for co-culture with MNCs. Cells were seeded at a density of 500,000 cells/ml and culture volume was 0.5 ml per well in 24-well plates. The cultures were incubated at 37 °C in a water saturated atmosphere containing 5% CO2/95% air and maintained in DMEM (Invitrogen) supplemented with 15% FBS (Invitrogen) for the first week and 10% FBS for the rest of the growth period. Astrocytes normally reached the stage of confluence 11–14 days after plating. Experiments were performed in triplicate using different batches of 3-week-old cell cultures. This procedure yielded cultures that showed 95% immunoreactivity for glial fibrillary acidic protein.

Oxygen and Glucose Deprivation and Co-Culture with MNCs When primary astrocytes reached the desired confluence, they were exposed to combined oxygen and glucose deprivation (OGD) to simulate the hypoxic conditions of acute ischemic stroke in vitro as we previously reported [26]. In brief, cultures were replaced with serum- and glucose-free medium then placed in a Billups-Rothenberg modular incubator chamber (Del Mar, San Diego, CA, USA), which was flushed for 5 min with 95% nitrogen and 5% CO2 and then sealed (hypoxia). The chamber was placed in a water-jacketed incubator (Forma scientific USA) at 37 °C for 45 min. After OGD, the maternal MNCs suspended in normal media were seeded into the well or into the upper chamber (0.4 μm, Corning, USA) of 24-transwell plate at a ratio of 1:10 (MNCs:Astrocytes) and co-cultured for 24 h. Normal media acted as a vehicle control and was added alone to the upper chamber for wells without astrocytes. Control glucose-containing normoxic cultures were incubated for the same periods of time at 37 °C in humidified 95% air and 5% CO2.

Western Blot Assay

Brain tissues were collected after intra-cardial perfusion with ice-cold PBS at day 3 after MCAo. The injured ipsilateral hemisphere was homogenized on ice in radioimmunoprecipitation assay (RIPA) buffer (Invitrogen, USA) containing a 1:100 (*v*/*v*) ratio of protease and phosphatase inhibitor cocktail (Roche, Tucson, AZ, USA). Cultured astrocytes were collected from 6 glass coverslips in 24-well plates after washing with PBS twice followed by lysis in 100 μl/well of the same lysis buffer. The protein concentration of each sample was determined using the Bicinchoninic Acid Assay (Sigma-Aldrich). Fifty micrograms of protein was separated on a 4–12% gradient sodium dodecyl sulfate–polyacrylamide gel electrophoresis (SDS-PAGE) gel using a Novex Mini Cell system (Invitrogen). The proteins were transferred onto a polyvinylidene fluoride membrane (Invitrogen) using the Novex Mini Cell system. Membranes were blocked (5% nonfat milk, 0.1% TWEEN-20 in Tris-buffered saline, pH 7.6) at room temperature for 2 h and incubated with primary antibodies overnight at 4 °C as reported [15]. The primary rabbit anti-rat antibodies were used as follows: anti-MMP3 (1:1000, Abcam), anti-p-JAK2 (1:2000, Santa Cruz), anti-p-STAT3 (1:2000, Santa Cruz), and rabbit anti-rat β-actin (1:2000, Santa Cruz) were used as a loading control. Horseradish peroxidase-conjugated monoclonal antibodies (eBioscience, USA) to rabbit were used as secondary antibodies, and membranes were then incubated for 1 h at room temperature. Immunoreactive bands were visualized using an enhanced chemiluminescence system (GE Healthcare) according to the manufacturer's protocol. X-ray films were scanned and then analyzed with ImageJ for densitometric analyses.

Statistical Analysis

Data are presented as the mean ± standard deviation. Densitometric quantitation of immunoblotting images was performed using ImageJ (National Institutes of Health). For comparison between two groups, significance level was determined by *t* test or by Mann–Whitney *U* test. For comparison among multiple groups, the one-way analysis of variance (ANOVA) followed by the post hoc Tukey–Kramer test was used to determine the level of significance. Statistical significance was set at $p < 0.05$ level. The statistical analysis was performed by Sigma Blot 11.0.

Results

Mortality

Complexity associated with embolic stroke model is well documented. Mortality rates tend to be high in this model [22]. In the present study, 90 rats were employed. Out of them, 4 rats were excluded because of the failure of MCAo and 32 rats did not survive to the end of experiments. Between the MNC treatment group and saline control, there was no significant difference in mortality.

MNC Treatment Did Not Reduce the Incidence of HT After t-PA Treatment

At day 3 after MCAo followed by t-PA treatment, there was visible hemorrhagic transformation in the local cerebral region. HT occurred either in the infarcted core or in the peri-infarct region. The incidence of visible HT after t-PA treatment was

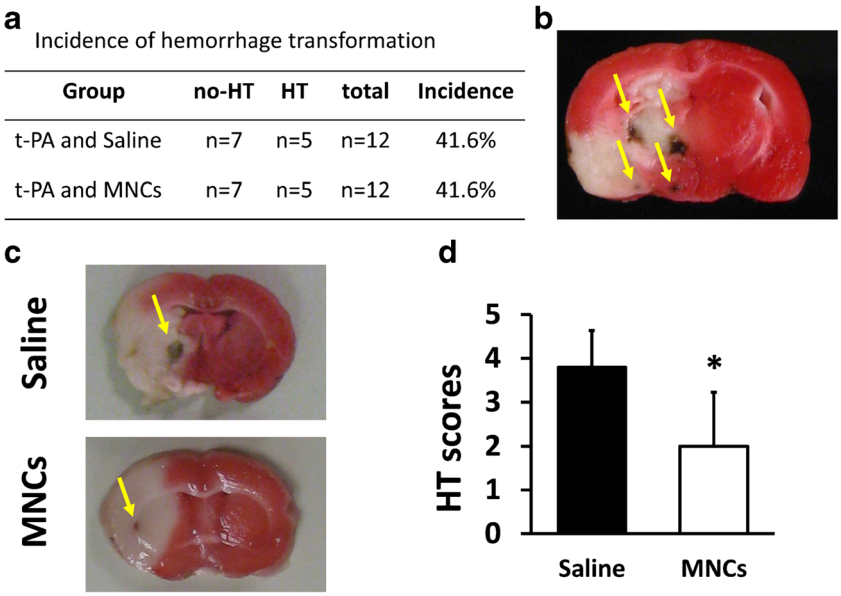

Fig. 2 t-PA treatment leads to HT and MNC treatment reduces the HT severity. **a** Table showing the HT incidence rate in two groups. **b** A representative picture showing HT occurring in different regions of the brain. **c** A representative picture showing MNC treatment causing reduction in severity of HT. **d** Bar graph showing significant reduction of HT scores after MNC treatment. *$p = 0.027$, compared to saline, $n = 5$ in each group

41.6% (5 out of 12 rats per group) in both groups. Treatment with MNCs did not alter the incidence, compared to saline control (Fig. 2a, b). We categorized hemorrhagic transformation into four subtypes using criteria from human study [22, 23]. We found that, in the saline group, 2/5 had HI-1, 2/5 had HI-2, and 1/5 had PH-1, while in the MNC group, 3/5 had HI-1, 2/5 had HI-2, and none of the subjects had parenchymal hematoma.

MNC Treatment Improved the Hemorrhage Severity Induced by t-PA After MCAo

Given that MNCs did not alter the incidence of HT induced by t-PA treatment after MCAo, we further compared the severity of intracerebral hemorrhage between two groups. The severity of ICH was assessed as reported by Choudhri et al. [27] with some modifications: rat brains were cut to 6 sections with 2 mm thickness. TTC-stained sections were inspected and the degree of hemorrhage was given a score based on maximal hemorrhage diameter at single hemorrhagic spots or the summary of diameters from multiple hemorrhage spots measured on any of the sections using NIH ImageJ software. Following hemorrhage score was given based on severity: 1 = no hemorrhage; 2 = < 1 mm hemorrhage; 3 = 1 to 2 mm hemorrhage; 4 = 2 to 3 mm hemorrhage; and 5 = > 3 mm hemorrhage. We observed that MNC treatment group scored significantly less as compared with saline control (2 ± 1.22 vs 3.8 ± 0.84, respectively, $p = 0.027$) (Fig. 2c, d).

MNC Treatment Did Not Significantly Alter Lesion Size and Behavioral Deficits

As we observed MNCs reduced HT severity scores induced by t-PA treatment, we measured the absolute infarction sizes in both groups. Interestingly, MNCs did not show reduction of lesion size compared with saline group (115 ± 12.3 vs. 146 ± 17.2 mm^3, respectively, $p = 0.11$) (Fig. 3a, b). Furthermore, there were no differences in neurobiological deficits scores between the two groups at day 3 after MCAo with t-PA treatment (Fig. 3c).

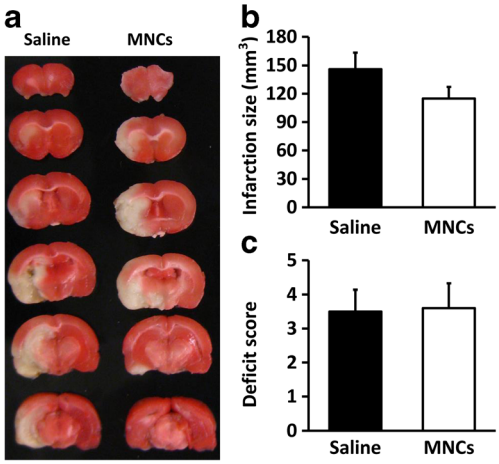

Fig. 3 **a** Representative TTC stained images showing the brain infarction in each brain section at 3 days after stroke and t-PA treatment. **b** Bar graph comparing infarction sizes between saline and MNC. **c** Bar graph showing neurological deficit score between saline and MNC-treated animals. No significant differences were observed in either infarction size or neurological deficits. $n = 12$ in each group

MNC Treatment Significantly Improved BBB Integrity After Stroke

As BBB permeability is reported to be associated with HT [28, 29], we quantified the BBB permeability between two groups with Evan's blue content from the ischemic hemisphere and contralateral hemisphere. As demonstrated in Fig. 4a, MCAo after t-PA treatment caused BBB disruption at day 3 after stroke. When these animals were treated with MNCs, there was a significant improvement in BBB integrity compared to saline treatment ($p = 0.033$).

MNC Treatment Significantly Reduced Brain, Serum MMP3 Level, and MMP3 Expression in GFAP Positive Astrocytes

MMP-3 plays a critical role in HT induced by t-PA treatment because of BBB disruption [30], we first detected MMP3 protein levels in the injured hemisphere from brains at day 3 after MCAo and MNC treatment. MNCs significantly reduced brain MMP3 level compared with saline treatment ($p = 0.014$) (Fig. 4b). We then measured MMP-3 levels in serum and found a significant decrease of MMP-3 level in MNC-treated group as compared to saline group ($p = 0.027$) (Fig. 4b). We have reported MNCs homing in the brain up to 7 days after stroke in our previous study in another ischemic stroke model [8, 14]. Thus, we then detect the grafted MNC potential interaction with astrocytes as astrocytes have been reported to play a pivotal role in an in vitro stroke model of the BBB [31]. We first observed that grafted MNCs (labeled with Q-tracker 655) homing in the peri-infarction area and had direct cell-cell touch with the processes of GFAP positive astrocytes (Fig. 4c). Furthermore, compared to the saline control group, MNC treatment significantly reduced MMP3 expression in GFAP positive astrocytes (Fig. 4d, e).

MNC Treatment After Stroke Significantly Changed the Serum Cytokine Levels Towards an Anti-Inflammatory Profile

Since the inflammatory responses play an important role in the potential mechanisms underlying BBB disruption after stroke, we measured serum IL-1β and IL-10 levels in both groups before MCAo and at 3 days after MCAo. Compared to saline, MNC treatment significantly reduced IL-1β level and

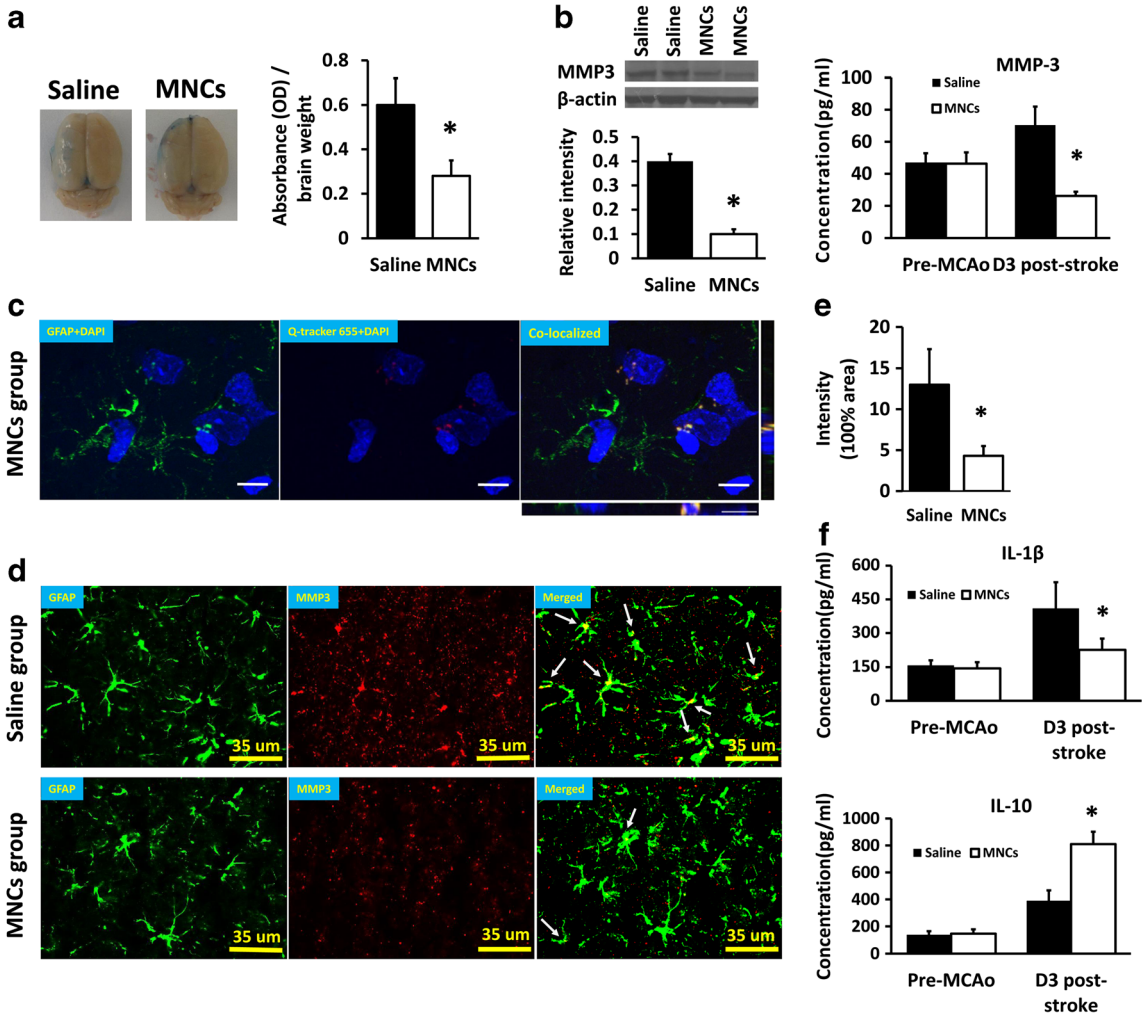

Fig. 4 MNCs improved BBB integrity after stroke. **a** Representative images of brain with Evan's blue staining in two groups. Bar graph showing that MNCs significantly reduced the Evan's blue leaking into brain tissue. *$p = 0.033$, compared to saline. $n = 6$ in each group. **b** Left: the representative immunoblots film scanning (upper) and bar graph (lower) exhibiting the relative quantitative expression levels of MMP-3 in the injured hemisphere from brains at day 3 after MCAo stroke. MNCs significantly reduced MMP3 level, compared to saline treatment. *$p = 0.014$, $n = 6$ in each group. Right: bar graph showing that MNC treatment significantly reduced the MMP3 level in serum. **c** Representative images from confocal microscope showing the direct contact of GFAP positive astrocyte processes on the grafted Q-track 655 labeled MNCs around. **d** Representative images showing the MMP3 expression in GFAP positive astocytes. Arrows pointed to the cells with co-localization of MMP3 and GFAP. **e** Bar graphs showing that MNC treatment significantly reduced the MMP3 expression in GFAP positive astrocytes. The density of co-localized fluorescence dots was calculated by ImageJ and compared. *$p = 0.044$, $n = 3$ in each group. **f** Bar graphs showing the levels of serum pro-inflammatory and anti-inflammatory cytokines in animals). Compared to pre-stroke, ischemic stroke followed by t-PA treatment increased IL-1β levels in serum at day 3 after stroke and MNCs significantly reduced this elevation. *$p = 0.011$, $n = 12$. IL-10 levels were further increased by MNCs. *$p = 0.045$, $n = 12$

increased IL-10 level in the serum after MCAo ($p = 0.011$, $p = 0.045$, respectively) (Fig. 4f), which was consistent with our previous findings in the suture MCAo models [14].

MMP-3 Secretion Was Decreased from Astrocytes Co-cultured with MNCs In Vitro Under OGD Conditions

Since we found that MNC treatment preserved the BBB when given after stroke following t-PA treatment in vivo, we further explored the potential mechanisms underlying these effects with experiments in vitro. We therefore cultured OGD-treated astrocytes to measure MMP-3 levels. Compared to astrocytes cultured in glucose-containing media under normoxic conditions, OGD-treated astrocytes released significant higher levels of MMP-3 (data not shown). Mixed co-culture of MNCs with astrocytes significantly attenuated MMP-3 levels from OGD-treated astrocytes ($p = 0.047$). However, in a transwell co-culture experiment, MNCs seeded in the upper chamber did not reduce MMP-3 levels released by OGD-treated astrocytes in the lower chamber (Fig. 5a).

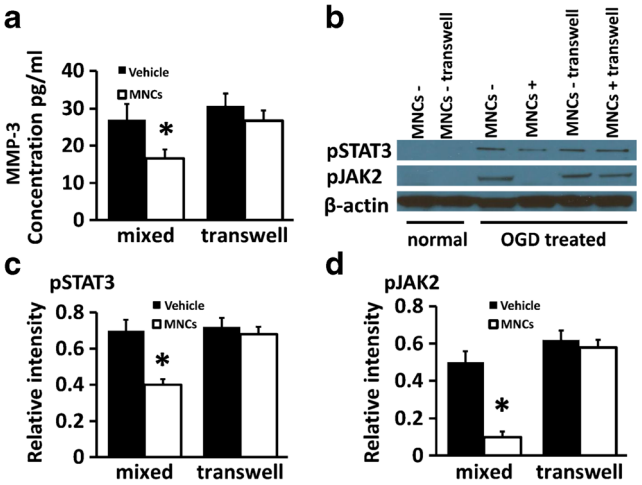

Fig. 5 MNCs decreased MMP-3 released by astrocytes in vitro after OGD by cell-to-cell direct contact via down-regulation of JAK/STAT3 signaling pathway. **a** Bar graphs showing that MNCs decrease MMP-3 levels in the media of MNCs co-cultured with astrocytes but not in the media of transwell. **b–d** Representative immunoblot film scanning from each group and bar graphs showing that MNCs down-regulate pJAK2/pSTAT3 expression level in astrocytes co-cultured directly with MNCs but not in the transwell. *$p = 0.007$ for pJAK2 and $p = 0.012$ for pSTAT3. Experiments were done in triplicate

Compared with astrocytes cultured in glucose-containing normoxic media, the p-JAK2/p-STAT3 level was increased in OGD-treated astrocytes. Mixed co-culture of MNCs with astrocytes significantly inhibited the activity of pJAK2 and pSTAT3 ($p = 0.012$ and $p = 0.007$, respectively), which might indicate that MNCs could reduce MMP3 levels through JAK-STAT pathway. However, transwell co-culture with MNCs did not alter the p-JAK2/p-STAT3 levels (Fig. 5b–d).

Discussion

Hemorrhage transformation is leakage of blood due to reperfused blood flow in the vasculature with disrupted BBB. HT is associated with increased mortality and morbidity. We employed an embolic MCAO model to simulate the conditions of hemorrhagic transformation after t-PA treatment which leads to a 10-fold increase in symptomatic intracranial hemorrhage transformation [32–34]. t-PA promotes reperfusion by degrading fibrin-based blood clots in the damaged ischemic brain [35, 36]. In our present study, we observed HT in both cortical and subcortical areas but not beyond the ischemic territory after t-PA treatment, which concords with previous reports [4, 37].

t-PA is also known to increase BBB permeability and play an important role in MMPs, PDGF-CC, and LRP receptor signaling [38]. The hypoperfusion and hyperemia within a previously occluded vessel can cause rapid BBB damage [25]. Since MNCs are being tested in clinical trials in patients with acute ischemic stroke and they have been reported to reduce BBB permeability in TBI [18] and ICH stroke model [15], we sought to determine the effects of MNCs on HT in an embolic stroke model in the context of t-PA treatment. In the present study, MNCs were given at 3 h after MCAo and 2 h after t-PA administration. In this time period, the early BBB damage by MCAo has occurred and the HT induced by t-PA should have occurred. It is likely that this time gap in administration of MNCs was the reason we did not see a change in incidence of HT by t-PA treatment.

We observed that the vascular leakage was reduced after MNC treatment suggesting that the BBB permeability is reduced as compared to that after stroke. There could be multiple reasons behind the beneficial effects of MNCs on BBB. First, our previous studies have shown that MNCs reduce the inflammatory response after stroke. In addition, MNCs modulate the immune response from the spleen as well as restores spleen mass [39]. Previous studies have shown that BBB permeability is increased by release of CD8+ lymphocytes after splenic contraction [40]. A plausible hypothesized mechanism of improved BBB integrity could be because of positive regulation of splenic inflammatory response after MNC treatment which provides an overall pro-regenerative environment. Second, BBB permeability is also affected by the secondary damage of reperfusion, which is associated with brain-derived factors including MMP-3, other proteases, vascular remodeling, and the inflammatory response as evidenced in our results. We observed that the severity of HT was reduced after MNC treatment. It is well known that matrix metalloproteinase dysregulation could be responsible for HT after t-PA [4]. Our study observed changes in the MMP3 levels after MNC treatment which could be responsible for reducing the severity of HT after MNC treatment. Since the focus of our present study was to observe the outcome of administering MNCs in an embolic stroke model in presence of t-PA and mechanistic studies were limited, we recommend that future mechanistic studies should be performed to explore the role of matrix metalloproteinase in severity of hemorrhagic transformation.

We have reported that MNCs gain access into brain [8, 14], which suggests potential effects of MNCs to modulate brain cells. Interestingly, this effect was not because of paracrine mechanisms or by release of trophic factors, but rather because of direct cell-to-cell contact between MNCs and astrocytes, seen by the fact that we see decrease in MMP3 levels only when MNCs and astrocytes are mixed co-cultured and not when co-cultured in transwell. These findings coupled with concurrent decrease in pJAK2 and pSTAT3 levels point towards involvement of JAK-STAT pathway. Previously, we have also reported that MNCs have the abilities to regulate neurotrophins, reduce brain edema, decrease pro-inflammatory responses systemically and locally in the brain, and protect the neurovascular unit in the suture stroke and ICH models [8, 14, 15]. In the present study, we observed that MNC treatment significantly reduced IL-1β and increased IL-10 levels in serum, which indicates that MNCs have an impact on down-regulation of pro-inflammatory responses and up-regulation of anti-

inflammatory responses in this embolic stroke model as well. MNCs also decreased serum, brain, and astrocytes MMP3 levels and improved BBB integrity. MMP-3 is a key metalloproteinases involved in BBB breakdown and HT after ischemic stroke [17, 41]. Reduction in MMP3 by MNCs treatment was consistent with what we have indicated previously in ICH model [15]. MMP-3 level could be increased as a result of stroke-related inflammation or through induction by t-PA. Furthermore, in the present study, we observed the direct contact of astrocyte processes to the homing grafted MNCs, providing the evidence of direct cell-cell contact in vivo to concur with our findings of in vitro study. Thus, the reduction in MMP3 levels after MNC treatment could be explained by decrease in stroke-related inflammation after administering MNCs. These findings, when combined with other results in our study, are indicative of pro-regenerative environment being created by MNCs in our embolic stroke model. Embolic stroke model which we used in our study is uniquely close to the clinical scenario where HT occurs after t-PA. To our knowledge, this is the first paper to report the effects of MNCs in an embolic stroke model, because of which our results carry high clinical significance.

A major limitation of this study is that the model used to harvest bone marrow for autologous MNCs around the administering t-PA is impractical to use clinically. That is the reason we focused this study on the MNC effects of hemorrhagic transformation caused by t-PA and did not extend the behavioral readouts and lesion size assessment beyond 3 days, although we previously reported the autologous MNC benefits of stroke recovery in a long-term observation period. However, our study provides a guideline that autologous MNCs given during the 3–4.5 h time window can exert neuroprotective effect. Our previous study showed that fresh vs cryopreserved cell therapy are equally effective after stroke [42]. Our results in this study provide a viable option to cryopreserve autologous MNCs for patients with high-risk factors of stroke. A major translational hurdle is to make these cell therapies work better. Combination therapies with death associated protein kinases (DAPK) have been suggested to improve stroke outcome [43]. Hydrogen sulfide has been shown to attenuate t-PA induced HT previously [44], an approach which could be combined with MNCs to further improve outcomes following t-PA administration. In addition, our study provides a direction for future mechanistic studies to explore how MNCs improve BBB integrity.

Acknowledgements This study was funded by grants: R01NS071127 and R21NS064316.

Compliance with Ethical Standards

Funding This study was funded by R01NS071127 and R21NS064316.

Conflict of Interest The authors declare that they have no conflict of interest.

Ethical Approval All animal experiments and surgical procedures were approved by the University of Texas Health Science Center Animal Welfare Committee and followed NIH guidelines and regulations.

This article does not contain any studies with human participants performed by any of the authors.

References

1. Kastrup A, Groschel K, Ringer TM, Redecker C, Cordesmeyer R, Witte OW, et al. Early disruption of the blood-brain barrier after thrombolytic therapy predicts hemorrhage in patients with acute stroke. Stroke. 2008;39(8):2385–7. https://doi.org/10.1161/STROKEAHA.107.505420.
2. Dijkhuizen RM, Asahi M, Wu O, Rosen BR, Lo EH. Rapid breakdown of microvascular barriers and subsequent hemorrhagic transformation after delayed recombinant tissue plasminogen activator treatment in a rat embolic stroke model. Stroke. 2002;33(8):2100–4.
3. Neumann-Haefelin C, Brinker G, Uhlenkuken U, Pillekamp F, Hossmann KA, Hoehn M. Prediction of hemorrhagic transformation after thrombolytic therapy of clot embolism: an MRI investigation in rat brain. Stroke. 2002;33(5):1392–8.
4. Zhang J, Yang Y, Sun H, Xing Y. Hemorrhagic transformation after cerebral infarction: current concepts and challenges. Ann Transl Med. 2014;2(8):81. https://doi.org/10.3978/j.issn.2305-5839.2014.08.08.
5. Rodriguez-Frutos B, Otero-Ortega L, Gutierrez-Fernandez M, Fuentes B, Ramos-Cejudo J, Diez-Tejedor E. Stem cell therapy and administration routes after stroke. Transl Stroke Res. 2016;7(5):378–87. https://doi.org/10.1007/s12975-016-0482-6.
6. Iihoshi S, Honmou O, Houkin K, Hashi K, Kocsis JD. A therapeutic window for intravenous administration of autologous bone marrow after cerebral ischemia in adult rats. Brain Res. 2004;1007(1–2):1–9. https://doi.org/10.1016/j.brainres.2003.09.084.
7. Giraldi-Guimardes A, Rezende-Lima M, Bruno FP, Mendez-Otero R. Treatment with bone marrow mononuclear cells induces functional recovery and decreases neurodegeneration after sensorimotor cortical ischemia in rats. Brain Res. 2009;1266:108–20. https://doi.org/10.1016/j.brainres.2009.01.062.
8. Yang B, Strong R, Sharma S, Brenneman M, Mallikarjunarao K, Xi X, et al. Therapeutic time window and dose response of autologous bone marrow mononuclear cells for ischemic stroke. J Neurosci Res. 2011;89(6):833–9. https://doi.org/10.1002/jnr.22614.
9. Hess DC, Wechsler LR, Clark WM, Savitz SI, Ford GA, Chiu D, et al. Safety and efficacy of multipotent adult progenitor cells in acute ischaemic stroke (MASTERS): a randomised, double-blind, placebo-controlled, phase 2 trial. Lancet Neurol. 2017;16(5):360–8. https://doi.org/10.1016/S1474-4422(17)30046-7.
10. Moniche F, Rosado-de-Castro PH, Escudero I, Zapata E, de la Torre Laviana FJ, Mendez-Otero R, et al. Increasing dose of autologous bone marrow mononuclear cells transplantation is related to stroke outcome: results from a pooled analysis of two clinical trials. Stem Cells Int. 2016;2016:8657173. https://doi.org/10.1155/2016/8657173.
11. Moniche F, Escudero I, Zapata-Arriaza E, Usero-Ruiz M, Prieto-Leon M, de la Torre J, et al. Intra-arterial bone marrow mononuclear cells (BM-MNCs) transplantation in acute ischemic stroke (IBIS trial): protocol of a phase II, randomized, dose-finding, controlled multicenter trial. Int J Stroke. 2015;10(7):1149–52. https://doi.org/10.1111/ijs.12520.
12. Prasad K, Sharma A, Garg A, Mohanty S, Bhatnagar S, Johri S, et al. Intravenous autologous bone marrow mononuclear stem cell

therapy for ischemic stroke: a multicentric, randomized trial. Stroke. 2014;45(12):3618–24. https://doi.org/10.1161/STROKEAHA.114.007028.
13. Savitz SI, Misra V, Kasam M, Juneja H, Cox CS Jr, Alderman S, et al. Intravenous autologous bone marrow mononuclear cells for ischemic stroke. Ann Neurol. 2011;70(1):59–69. https://doi.org/10.1002/ana.22458.
14. Yang B, Migliati E, Parsha K, Schaar K, Xi X, Aronowski J, et al. Intra-arterial delivery is not superior to intravenous delivery of autologous bone marrow mononuclear cells in acute ischemic stroke. Stroke. 2013;44(12):3463–72. https://doi.org/10.1161/STROKEAHA.111.000821.
15. Suda S, Yang B, Schaar K, Xi X, Pido J, Parsha K, et al. Autologous bone marrow mononuclear cells exert broad effects on short- and long-term biological and functional outcomes in rodents with Intracerebral hemorrhage. Stem Cells Dev. 2015;24(23):2756–66. https://doi.org/10.1089/scd.2015.0107.
16. Yang Y, Rosenberg GA. Blood-brain barrier breakdown in acute and chronic cerebrovascular disease. Stroke. 2011;42(11):3323–8. https://doi.org/10.1161/STROKEAHA.110.608257.
17. Gurney KJ, Estrada EY, Rosenberg GA. Blood-brain barrier disruption by stromelysin-1 facilitates neutrophil infiltration in neuroinflammation. Neurobiol Dis. 2006;23(1):87–96. https://doi.org/10.1016/j.nbd.2006.02.006.
18. Bedi SS, Walker PA, Shah SK, Jimenez F, Thomas CP, Smith P, et al. Autologous bone marrow mononuclear cells therapy attenuates activated microglial/macrophage response and improves spatial learning after traumatic brain injury. J Trauma Acute Care Surg. 2013;75(3):410–6. https://doi.org/10.1097/TA.0b013e31829617c6.
19. Shi Y, Leak RK, Keep RF, Chen J. Translational stroke research on blood-brain barrier damage: challenges, perspectives, and goals. Transl Stroke Res. 2016;7(2):89–92. https://doi.org/10.1007/s12975-016-0447-9.
20. Fan X, Qiu J, Yu Z, Dai H, Singhal AB, Lo EH, et al. A rat model of studying tissue-type plasminogen activator thrombolysis in ischemic stroke with diabetes. Stroke. 2012;43(2):567–70. https://doi.org/10.1161/STROKEAHA.111.635250.
21. Korninger C, Collen D. Studies on the specific fibrinolytic effect of human extrinsic (tissue-type) plasminogen activator in human blood and in various animal species in vitro. Thromb Haemost. 1981;46(2):561–5.
22. Fiorelli M, Bastianello S, von Kummer R, del Zoppo GJ, Larrue V, Lesaffre E, et al. Hemorrhagic transformation within 36 hours of a cerebral infarct: relationships with early clinical deterioration and 3-month outcome in the European cooperative acute stroke study I (ECASS I) cohort. Stroke. 1999;30(11):2280–4.
23. Fagan SC, Lapchak PA, Liebeskind DS, Ishrat T, Ergul A. Recommendations for preclinical research in hemorrhagic transformation. Transl Stroke Res. 2013;4(3):322–7. https://doi.org/10.1007/s12975-012-0222-5.
24. Bederson JB, Pitts LH, Tsuji M, Nishimura MC, Davis RL, Bartkowski H. Rat middle cerebral artery occlusion: evaluation of the model and development of a neurologic examination. Stroke. 1986;17(3):472–6.
25. Zhuang Z, Yang B, Theus MH, Sick JT, Bethea JR, Sick TJ, et al. EphrinBs regulate D-serine synthesis and release in astrocytes. J Neurosci. 2010;30(47):16015–24. https://doi.org/10.1523/JNEUROSCI.0481-10.2010.
26. Sharma S, Yang B, Strong R, Xi X, Brenneman M, Grotta JC, et al. Bone marrow mononuclear cells protect neurons and modulate microglia in cell culture models of ischemic stroke. J Neurosci Res. 2010;88(13):2869–76. https://doi.org/10.1002/jnr.22452.
27. Choudhri TF, Hoh BL, Solomon RA, Connolly ES Jr, Pinsky DJ. Use of a spectrophotometric hemoglobin assay to objectively quantify intracerebral hemorrhage in mice. Stroke. 1997;28(11):2296–302.
28. Leigh R, Jen SS, Hillis AE, Krakauer JW, Barker PB. Stir et al. pretreatment blood-brain barrier damage and post-treatment intracranial hemorrhage in patients receiving intravenous tissue-type plasminogen activator. Stroke. 2014;45(7):2030–5. https://doi.org/10.1161/STROKEAHA.114.005249.
29. Khatri R, McKinney AM, Swenson B, Janardhan V. Blood-brain barrier, reperfusion injury, and hemorrhagic transformation in acute ischemic stroke. Neurology. 2012;79(13 Suppl 1):S52–7. https://doi.org/10.1212/WNL.0b013e3182697e70.
30. Suzuki Y, Nagai N, Umemura K, Collen D, Lijnen HR. Stromelysin-1 (MMP-3) is critical for intracranial bleeding after t-PA treatment of stroke in mice. J Thromb Haemost. 2007;5(8):1732–9. https://doi.org/10.1111/j.1538-7836.2007.02628.x.
31. Neuhaus W, Gaiser F, Mahringer A, Franz J, Riethmuller C, Forster C. The pivotal role of astrocytes in an in vitro stroke model of the blood-brain barrier. Front Cell Neurosci. 2014;8:352. https://doi.org/10.3389/fncel.2014.00352.
32. Tissue plasminogen activator for acute ischemic stroke. The National Institute of Neurological Disorders and Stroke rt-PA stroke study group. N Engl J Med 1995;333(24):1581–7. doi: https://doi.org/10.1056/NEJM199512143332401.
33. Hacke W, Kaste M, Fieschi C, Toni D, Lesaffre E, von Kummer R, et al. Intravenous thrombolysis with recombinant tissue plasminogen activator for acute hemispheric stroke. The European cooperative acute stroke study (ECASS). JAMA. 1995;274(13):1017–25.
34. Intracerebral hemorrhage after intravenous t-PA therapy for ischemic stroke. The NINDS t-PA stroke study group. Stroke 1997;28(11):2109–18.
35. Asahi M, Asahi K, Wang X, Lo EH. Reduction of tissue plasminogen activator-induced hemorrhage and brain injury by free radical spin trapping after embolic focal cerebral ischemia in rats. J Cereb Blood Flow Metab. 2000;20(3):452–7. https://doi.org/10.1097/00004647-200003000-00002.
36. Brinker G, Pillekamp F, Hossmann KA. Brain hemorrhages after rt-PA treatment of embolic stroke in spontaneously hypertensive rats. Neuroreport. 1999;10(9):1943–6.
37. Dijkhuizen RM, Asahi M, Wu O, Rosen BR, Lo EH. Delayed rt-PA treatment in a rat embolic stroke model: diagnosis and prognosis of ischemic injury and hemorrhagic transformation with magnetic resonance imaging. J Cereb Blood Flow Metab. 2001;21(8):964–71. https://doi.org/10.1097/00004647-200108000-00009.
38. Jickling GC, Liu D, Stamova B, Ander BP, Zhan X, Lu A, et al. Hemorrhagic transformation after ischemic stroke in animals and humans. J Cereb Blood Flow Metab. 2014;34(2):185–99. https://doi.org/10.1038/jcbfm.2013.203.
39. Yang B, Hamilton JA, Valenzuela KS, Bogaerts A, Xi X, Aronowski J, et al. Multipotent adult progenitor cells enhance recovery after stroke by modulating the immune response from the spleen. Stem Cells. 2017;35(5):1290–302. https://doi.org/10.1002/stem.2600.
40. Walker PA, Shah SK, Jimenez F, Gerber MH, Xue H, Cutrone R, et al. Intravenous multipotent adult progenitor cell therapy for traumatic brain injury: preserving the blood brain barrier via an interaction with splenocytes. Exp Neurol. 2010;225(2):341–52. https://doi.org/10.1016/j.expneurol.2010.07.005.
41. Sashindranath M, Sales E, Daglas M, Freeman R, Samson AL, Cops EJ, et al. The tissue-type plasminogen activator-plasminogen activator inhibitor 1 complex promotes neurovascular injury in brain trauma: evidence from mice and humans. Brain. 2012;135(Pt 11):3251–64. https://doi.org/10.1093/brain/aws178.
42. Yang B, Parsha K, Schaar K, Satani N, Xi X, Aronowski J, et al. Cryopreservation of bone marrow mononuclear cells alters their

viability and subpopulation composition but not their treatment effects in a rodent stroke model. Stem Cells Int. 2016;2016: 5876836. https://doi.org/10.1155/2016/5876836.

43. Glover LE, Tajiri N, Weinbren NL, Ishikawa H, Shinozuka K, Kaneko Y, et al. A step-up approach for cell therapy in stroke: translational hurdles of bone marrow-derived stem cells. Transl Stroke Res. 2012;3(1):90–8. https://doi.org/10.1007/s12975-011-0127-8.
44. Liu H, Wang Y, Xiao Y, Hua Z, Cheng J, Jia J. Hydrogen sulfide attenuates tissue plasminogen activator-induced cerebral hemorrhage following experimental stroke. Transl Stroke Res. 2016;7(3):209–19. https://doi.org/10.1007/s12975-016-0459-5.